Article

Construction of L-Asparaginase Stable Mutation for the Application in Food Acrylamide Mitigation

Bing Yuan [1,†], Pengfei Ma [2,†], Yuxuan Fan [1], Bo Guan [1], Youzhen Hu [1], Yan Zhang [1], Wenli Yan [1], Xu Li [1,*] and Yongqing Ni [1,*]

1   School of Food Science and Technology, Shihezi University, Shihezi 832003, China; ybiice@163.com (B.Y.); sprinklefan@163.com (Y.F.); guanbo@shzu.edu.cn (B.G.); yzhu@shzu.edu.cn (Y.H.); zhangyanzqgh@163.com (Y.Z.); wenliyan62@sina.com (W.Y.)
2   Changji Hui Autonomous Prefecture Institute for Drug Control, Changji 831100, China; mpf2551241@163.com
*   Correspondence: leeluok@163.com (X.L.); niyqlzu@sina.com (Y.N.)
†   These authors contributed equally to this work.

Abstract: Acrylamide, a II A carcinogen, widely exists in fried and baked foods. L-asparaginase can inhibit acrylamide formation in foods, and enzymatic stability is the key to its application. In this study, the *Escherichia coli* L-asparaginase (ECA) stable variant, D60W/L211R/L310R, was obtained with molecular dynamics (MD) simulation, saturation mutation, and combinatorial mutation, the half-life of which increased to 110 min from 60 min at 50 °C. Furthermore, the working temperature (maintaining the activity above 80%) of mutation expanded from 31 °C–43 °C to 35 °C–55 °C, and the relative activity of mutation increased to 82% from 65% at a pH range of 6–10. On treating 60 U/mL and 100 U/g flour L-asparaginase stable mutant (D60W/L211R/L310R) under uncontrolled temperature and pH, the acrylamide content of potato chips and bread was reduced by 66.9% and 51.7%, which was 27% and 49.9% higher than that of the wild type, respectively. These results demonstrated that the mutation could be of great potential to reduce food acrylamide formation in practical applications.

Keywords: L-asparaginase; stability; mutation; acrylamide; food safety

1. Introduction

Potatoes and flour, two of the most important staple foods, are rich in carbohydrates. However, while these high-carbohydrate foods are processed at high temperatures (above 120 °C), a large amount of acrylamide is formed due to the Maillard reaction between reducing sugars and amino acids [1]. The acrylamide content in microwaved snacks and French fries, respectively, reached 20,336 μg/kg and 10,712 μg/kg [2,3], which far exceeded the limit of acrylamide in daily drinking water set by the World Health Organization by 0.5 μg/L, triggering international health alerts.

Some strategies such as raw material selection, processing optimization, addition of plant extracts, and enzymatic treatment were researched to reduce the acrylamide content in food [4–7]. Among these, L-asparaginase (EC 3.5.1.1), which was found to effectively inhibit the acrylamide formation in food by removing the acrylamide precursor (L-asparagine) without changing the food senses [8–11], has attracted extensive attention. On a laboratory scale, different sources of L-asparaginase have been used to inhibit acrylamide formation under restricted reaction conditions [2,12–14]. Wang et al. (2021) pretreated French fries with 10 U/mL *Palaeococcus ferrophilus* L-asparaginase at 85 °C for 10 min to reduce the acrylamide content by 80% [2]. Farahat et al. (2020) reduced acrylamide in French fries by 82% using 20 U/mL *Cobetia amphilecti* L-asparaginase at 40 °C for 30 min [15]. Ran et al. (2017) used *Paenibacillus barengoltzii* L-asparaginase to pretreat French fries and mooncake at 45 °C for 20 and 60 min, and found that the acrylamide content was lowered by 86% and 52%, respectively [13]. Commercial L-asparaginase (10 U/mL; Acrylaway® L-asparaginase)

was used to pretreat French fries at 75 °C for 10 min to reduce the acrylamide content by 60% [16].

Many investigations have been conducted to inhibit acrylamide formation in food with L-asparaginase on a laboratory scale, but few have been performed on an industrial scale [9]. Operational temperature, pH, and time are the crucial parameters for the successful application of L-asparaginase on an industrial scale. Hence, L-asparaginase, with better stability, wider action temperature, and pH, has more industrial application potential. In this study, the key residues of *E. coli* L-asparaginase (ECA) were identified by molecular dynamics (MD) simulation. Then, the stability of ECA was improved through saturation and compound mutations, and its application temperature and pH were expanded. Finally, we evaluated its application effect in inhibiting acrylamide formation in potato chips and bread under restricted and non-restricted reaction conditions.

2. Materials and Methods

2.1. Strains, Plasmids, and Chemicals

E. coli BL21 was used as the host strain for gene cloning and expression. The shuttle expression plasmid pET-28a was used for expression and mutagenesis studies. All strains and plasmids were preserved in our laboratory. The restriction enzymes, PrimeSTAR® HS DNA Polymerase and T4 DNA ligase, were purchased from TaKaRa Bio Co. (Dalian, China), and the Mini Plasmid Rapid Isolation Kit and Mini DNA Rapid Purification Kit were obtained from Sangon Biotech Co., Ltd. (Shanghai, China). A HisTrapTM HP column was purchased from GE Healthcare, Inc. (Little Chalfont, Buckinghamshire, UK). All other high-grade chemicals were commercially sourced.

2.2. Construction of Recombinant Strains

The plasmid pET-28a-ansE harboring the ECA gene, obtained from our lab stock [17], was used as the template for cloning mutation genes. With overlap extension PCR, site-saturation mutagenesis was introduced using corresponding primers (Table S1). Using pET-28a-D60W (constructing with site-saturation mutagenesis and harboring the ECA asparaginase mutation D60W gene) as the template, a combinatorial mutant D60W/L211R/L310R gene was constructed by two rounds of PCR using primer pairs F4 and R4 and F5 and R5. All mutations were linked to linearized pET-28a and transferred into *E. coli* BL21 for gene cloning expression. All recombinant plasmids were sequenced by Sangon Biotech Co., Ltd. (Shanghai, China).

2.3. Expression, Purification, and Activity Assay

The expression of ECA and its mutations in *E.coli* BL21 were performed as described by Zhang [18]. Recombinant *E. coli* BL21 were cultured at 37 °C to OD = 1.0 (approximately 3 h) and were induced with 1 mM IPTG, after which time the culture was incubated for 10 h at 16 °C. The cell paste was suspended in Tris-HCl buffer (pH 8.0) and disrupted on ice by sonication to obtain the intracellular proteins (crude enzyme).

The purification and property determination of all proteins were carried out as described in our previous study [17,19]. Ni^{2+}-affinity chromatography and an AKTA purifier system (GE Healthcare, Danderyd, Sweden) were used to purify the crude enzyme. The crude enzyme was loaded onto a 1-mL HisTrapTM HP column with Binding Buffer (0.02 M Tris-HCl buffer and 0.5 M NaCl, pH 7.4) with a 0.5 mL/min loading rate. L-asparaginase was eluted at 1 mL/min with a linear gradient of imidazole concentrations ranging from 0 to 0.5 M. Then, the purified enzyme was dialyzed with Tris-HCl buffer (0.05 M, pH 7.0) to remove imidazole and recycled for SDS-PAGE analysis. The enzyme with only a single SDS-PAGE target band was the purified enzyme at the end of the process.

The activity of ECA II and its mutations were assayed as described by Li [17,20]. The reaction mixture (1 mL) containing L-asparagine (25 mM) and Tris-HCl (50 mM, pH 8.0) was preheated at optimum temperature. Then, 100 μL of enzyme solution was added and reacted with the substrate for 10 min. One hundred μL of 15% trichloroacetic acid (TCA) was

used to stop the reaction. The reaction mixture was centrifuged at $20,000 \times g$, mixed gently with 200 μL of the clear supernatant, 4.8 mL of deionized water and 200 μL of Nessler's reagent, and the amount of ammonia released was measured. All measurements were performed spectrophotometrically at 450 nm. TCA and enzyme solution were successively added to the reaction mixture and were used as a blank during the spectrophotometric enzyme activity assays. One unit of L-asparaginase activity was defined as the amount of enzyme required to release 1 μmol of ammonia per minute under assay conditions.

2.4. Determination of Optimum Temperature, Optimum pH, and Thermal Stability

The optimum temperature of L-asparaginase was examined using 50 mM Tris-HCl buffer (pH 7.5) with temperatures ranging from 20 to 60 °C. The optimum pH was measured by assaying the enzyme activity at various pH values (0.05 M acetate buffer, pH 4.0–6.0; 0.05 M phosphate buffer, pH 6.0–7.0; 0.05 M Tris-HCl buffer, pH 7.0–9.0; and 0.05 M glycine-NaOH buffer, pH 9.0–10.0) at optimum temperature. The thermal stability of L-asparaginase was determined by incubating the enzyme in Tris-HCl buffer (50 mM, pH 7.0) for 15–120 min at 50 °C. After incubation, the protein was refolded on ice for 15 min, and the residual enzyme activity was measured at optimum temperature and pH.

2.5. Structure Modeling and MD Simulation

The ECA crystal conformation (PDB ID: 6PAB) as a template [21] and ECA mutation model were acquired by homology modeling using SWISS-MODEL (http://swissmodel.expasy.org/, accessed on 20 March 2022). The molecular structures of all proteins were analyzed using the Program PyMOL [22].

MD simulations were conducted using GROMACS software in a similar manner as in our previous study, to analyze the stability of protein structures [17]. The protein model was immersed in a dodecahedron box, and the distance between any protein atom and the edge of the box was set at >1.2 nm. Following the addition of Na^+ (0.15 M) to balance the negative charges, the system was minimized using the steepest descent method. After MD simulations of ECA conducted at 310 K and 323 K reference temperatures for 30 ns, the root mean square fluctuation (RMSF) values of residues were calculated.

2.6. Application of ECA in French Fries and Bread

The treatment of potatoes was modified based on the study of Farahat et al. [15]. Potatoes (Fovorita, pH 7.3) and bread flour (pH 6.4) were purchased from the local supermarket in Shihezi, Xinjiang Province. The potatoes were peeled and cut into strips ($0.5 \times 0.5 \times 10$ cm^3), and then the strips were immersed in distilled water for 2 min to remove the starch from the surface. To investigate the effect of enzyme on the acrylamide formation in French fries under different conditions, the raw fries were submerged in an enzyme solution (50 mM, pH 7.5 Tris-HCl buffer or tap water, with enzyme concentrations of 10, 20, 40, 60, and 80 U/mL) at 37 °C, 45 °C, and uncontrolled temperature for 20 min each, while the control group was submerged in a similar solution (50 mM, pH 7.5 Tris-HCl buffer or tap water) without the enzyme for 20 min. All samples were fried at 160 °C for 10 min in an electric fryer. After frying, the fries were cooled on a paper at an ambient temperature, and then the acrylamide was extracted for analysis.

The bread dough was prepared using flour (300 g), yeast (3 g), and an enzyme solution (200 g, 50 mM, pH 7.5 Tris-HCl buffer or tap water, with enzyme concentrations of 40, 60, 80, 100, and 120 U/g flour enzyme, and without enzyme as the control group). The dough was kneaded and allowed to rest for 60 min at different temperatures (37 °C, 45 °C, or room temperature). Finally, the bread dough was baked in an oven at 180 °C for 20 min. The bread was cooled at an ambient temperature, and then the acrylamide was extracted for analysis.

2.7. Assay of Concentration Assay

The acrylamide in French fries and bread was extracted by the method described by Wang et al. [2]. One gram of the crushed sample (French fries or bread) was accurately weighed in a 50-mL centrifuge tube, vortexed with 10 mL of hexane for 1 min and centrifuged at 10,000 *g* for 5 min at 4 °C, and the hexane layer was removed. The aforementioned operation was repeated thrice to get rid of the long-chain fatty acids from the sample. Thereafter, 10 mL of methanol, 500 µL of Carrez I (3.6 g potassium ferricyanide/100 mL ultrapure water), and 500 µL of Carrez II (7.2 g zinc sulfate/100 mL ultrapure water) were added to the centrifuge tube and shaken at 30 °C for 30 min. The homogenates were centrifuged at 10,000 *g* for 30 min at 4 °C, and the supernatant was filtered through 0.22-µm Millipore filters. The extracted samples were detected by high-performance liquid chromatography (HPLC) using a C18 chromatographic column (Atlantis TM, 150×2.1 mm^2) and a UV detector. The HPLC operating conditions included a mobile phase of 70% (*v/v*) methanol, UV wavelength set at 210 nm, injection volume of 20 µL, and a column temperature of 30 °C. Different concentrations of acrylamide (50–4000 g/L) were used as the reference for HPLC detection.

3. Results and Discussion

3.1. Identification of ECA Stability Key Domains

In our previous study, ECA was expressed by *E. coli* BL21, with a half-life of 6.2 h and 1 h at 37 °C and 50 °C, respectively [17]. The half-life of the enzyme was shortened by 5.2 h when the temperature increased by only 13 °C, which attracted our attention. MD software imparted significant guidance in analyzing enzyme's structural characteristics and rational design [23–26]. The GROMACS software effectively calculated the RMSF of protein amino acids at a simulated temperature and then showed the flexibility of the residue domain at different temperatures [27–30]. To find out why ECA was unstable at higher temperatures at a protein structure level, the RMSF of ECA residues were calculated at 37 °C and 50 °C based on the ECA crystal conformation (PDB ID: 6PAB) [21]. The RMSF of domains G57-T80, P202-K213, and N298-T311 increased by 1.01 nm, 1.00 nm, and 1.08 nm, respectively, which was much higher than the average RMSF increase of 0.60 nm (Supplementary Data and Figure 1A), indicating that these regions fluctuated greatly at higher temperatures.
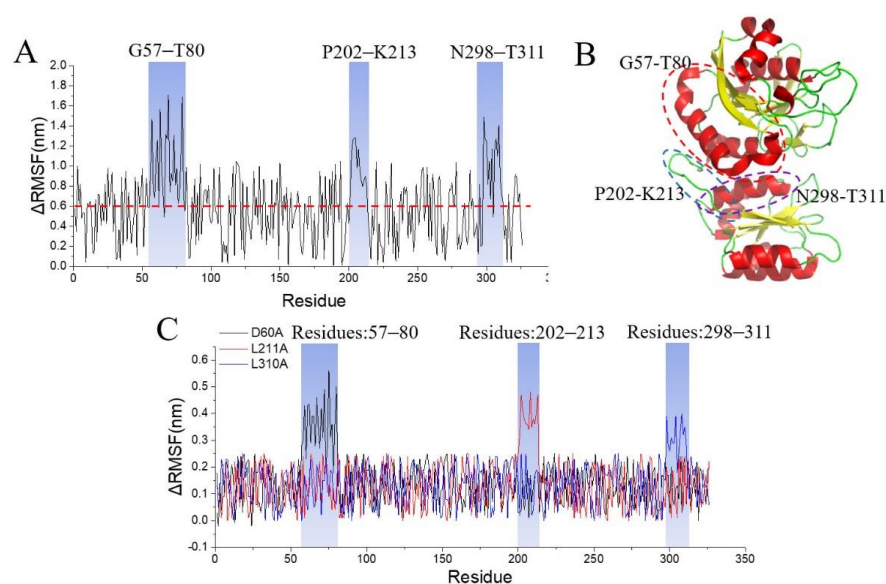

Figure 1. Molecular dynamics simulation and structural analysis of ECA. (**A**) RMSF value of ECA at 37 °C and 50 °C. (**B**) Stability key domains in ECA tertiary structure. G57-T80: the α-helix in red-dashed box; P202-K213: the loop in blue-dashed box; N298-T311: the α-helix in purple-dashed box. (**C**) ECA RMFS with "alanine scanning".

The subunit of L-asparaginase is composed of a large N-terminal and a small C-terminal, and the dimer assembly of the N- and C-terminals "head-to-tail" constitutes the basic functional unit [31–33]. As found in the ECA model (Figure 1B), at the interface of L-asparaginase subunit N- and C-terminals, domains G57-T80 and N298-T311 were, respectively, located as α-helix, and P202-K213 located as the link loop connecting the N- and C-terminals. These interface function domains (G57-T80, P202-K213, and N298-T311) fluctuated at 50 °C, which might be the reason for the sharp shortening of the protein's half-life at 50 °C than that at 37 °C, and were the key domains of thermal stability [29,34].

3.2. Identification of Stability Key Residues and Construction of Stability Mutation

To determine the unstable key residues in the three domains, these domains' residues (except for alanine) were computationally substituted with alanine (alanine scanning; if the original residue was alanine, it was replaced with glycine) at 50 °C [35]. As shown in the results (Supplementary Data and Figure 1C), the RMSF of the mutations D60A, L211A, and L310A showed a maximum rise in the domains G57-T80, P202-K213, and N298-T311, respectively. The results showed that D60, L211, and L310 might be the key residues for the ECA stability.

Saturation mutations were carried out to further verify the effect of these residues (D60, L211, and L310) on the ECA stability and improve the stability (Table 1). The thermal stability of mutations D60W, L211R, and L310R were improved, the half-life of the combinatorial mutant (D60W/L211R/L310R) was extended from 60 to 110 min at 50 °C, while other enzyme characteristics showed no significant changes (Table 1).

Table 1. The enzyme characteristics of ECAII and its mutations.

Enzyme	Optimum Temperature (°C)	$T_{(1/2, 50\,°C)}$ (Min)	Optimum pH	K_m (μM)	Specific Activity (U/mg)
ECA II	37	60 ± 5	7.5	18 ± 5	235 ± 21
D60W	40	85 ± 5	7.0	15 ± 6	245 ± 31
L211R	42	95 ± 5	7.5	24 ± 8	290 ± 33
L310R	40	80 ± 5	8.0	14 ± 6	217 ± 20
D60W/L211R/L310R	45	110 ± 10	7.5	26 ± 6	281 ± 29
D60A	35	40 ± 5	7.0	28	271 ± 29
D60I	37	50 ± 5	7.0	41	301 ± 41
D60V	37	60 ± 5	7.0	56	223 ± 21
D60F	40	75 ± 5	7.0	32	189 ± 31
D60M	37	60 ± 5	7.5	15	233 ± 33
D60Q	40	75 ± 5	7.5	66	199 ± 24
D60T	37	55 ± 5	7.0	90	211 ± 17
D60N	37	45 ± 5	7.0	55	273 ± 19
D60Y	40	70 ± 5	7.5	24	248 ± 24
D60E	37	60 ± 5	7.0	33	221 ± 44
L211G	35	40 ± 5	7.5	77	281 ± 37
L211A	35	45 ± 5	7.5	63	277 ± 21
L211I	37	55 ± 5	7.5	69	249 ± 11
L211V	37	45 ± 5	7.5	93	211 ± 18
L211P	40	75 ± 5	7.0	45	198 ± 55
L211F	40	65 ± 5	7.5	51	255 ± 23
L211W	37	65 ± 5	7.0	101	294 ± 36
L211S	40	60 ± 5	7.0	67	211 ± 19
L211T	37	45 ± 5	7.5	32	234 ± 12
L211N	37	55 ± 5	8.0	55	189 ± 11
L211D	40	65 ± 5	8.0	41	243 ± 28
L211E	40	70 ± 5	7.5	27	257 ± 31
L211K	40	70 ± 5	7.5	91	231 ± 37
L310A	37	45	7.5	33	221 ± 41
L310I	37	55	7.5	48	232 ± 21
L310P	40	70	7.5	19	203 ± 19

Table 1. *Cont.*

Enzyme	Optimum Temperature (°C)	$T_{(1/2,\ 50\ °C)}$ (Min)	Optimum pH	K_m (µM)	Specific Activity (U/mg)
L310F	40	75	8.0	36	199 ± 23
L310M	37	60	8.0	52	198 ± 41
L310W	40	65	8.0	20	188 ± 28
L310Q	37	50	7.5	13	236 ± 23
L310T	37	55	7.5	54	210 ± 31
L310C	37	50	7.5	33	179 ± 51
L310N	37	55	7.5	64	198 ± 31
L310Y	40	65	7.5	88	204 ± 42
L310K	37	60	7.5	91	218 ± 16
L310H	37	65	7.5	31	221 ± 12

To fully understand how the residue mutations D60W, L211R, and L310R affected the thermostability, the combinatorial mutant (D60W/L211R/L310R) was modeled using the crystal structure of ECA (PDB ID: 6PAB). As shown in Figure 2A, the 60th, 211th, and 310th residues were located in the key domains G57-T80, P202-K213, and N298-T311, respectively. After the 60th residue Asp was mutated into Trp, an additional hydrogen bond was formed with the 249th residue Leu on the adjacent subunit. Compared with L211, L211R formed additional hydrogen with Asp63 and Gln307 on G57-T80 and N298-T311, respectively. After the 310th residue, Leu mutated into Arg. Although the connection with the 307th residue was lost, an additional hydrogen bond was formed with the 306th residue Leu and 237th residue Asp. Meanwhile, the RMSF of site-mutations (D60W, L211R, and L310R) and combinatorial mutant (D60W/L211R/L310R) were calculated at 50 °C (Supplementary Data and Figure 2B). The RMSF of site-mutations D60, L211R, and L310R decreased by 0.15 nm, 0.20 nm, and 0.21 nm and the RMSF of their respective regions (G57-T80, P202-K213, and N298-T311) were, respectively, reduced by 0.19 nm, 0.32 nm, and 0.27 nm compared with the wild type. Furthermore, compared with the wild type, the RMSF of the combinatorial mutant (D60W/L211R/L310R) decreased by 0.21 nm, and its RMSF of G57-T80, P202-K213, and N298-T311 decreased by 0.28 nm, 0.26 nm, and 0.25 nm, respectively. These results suggested that all the three residue mutations formed more hydrogen bonds with nearby residues after mutation, which made the connection between the N- and C-terminals of ECA and the connection between the subunits more inseparable, and in turn made the protein structure more difficult to be destroyed. Hence, the thermostability of the combinatorial mutant was improved.

Considering that the extensive application without controlling the treatment temperature and pH was more favorable, we measured the relative activity in the temperature range of 10 °C–70 °C and pH range of 6–10 before and after mutation (Figure 3). Compared with the wild type, the working temperature (the temperature of relative activity > 80%) range of D60W/L211R/L310F was expanded from 31 °C–43 °C to 35 °C–55 °C. Meanwhile, at a pH range of 6–10, the relative activity of D60W/L211R/L310F remained above 82%, while that of the wild type was only 65%. The mutant D60W/L211R/L310F had more hydrogen bonds in the key domains and better stability [36–39], so it could remain stable under adverse conditions (such as high temperature or highly acidic alkaline conditions), which also indirectly widened its working conditions.
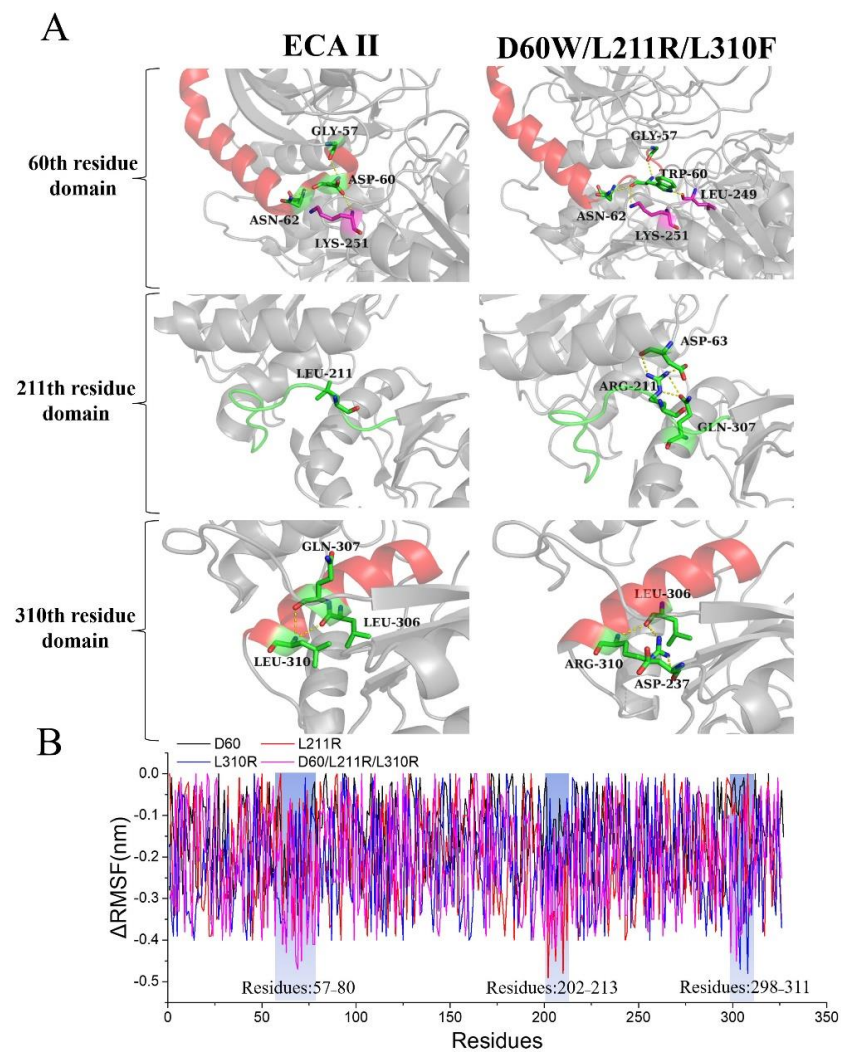
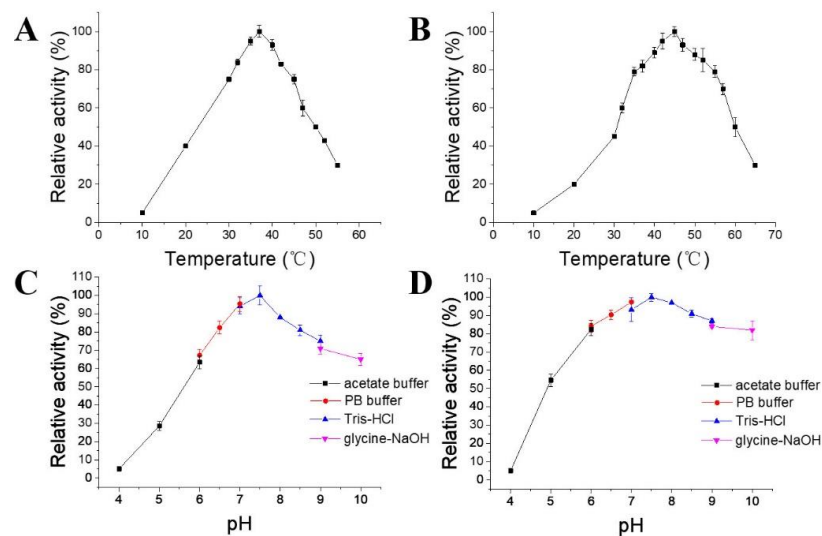**Figure 2.** Tertiary structure around ECA stability key residues (**A**) and the changes of RMSF between ECA and its mutants (**B**).

Figure 3. Activity of ECA and its mutation D60W/L211R/L310F at different temperatures and pH. (**A**,**B**) Activity of ECA (**A**) and its mutation D60W/L211R/L310F (**B**) at different temperatures. (**C**,**D**): Activity of ECA (**C**) and its mutation D60W/L211R/L310F (**D**) at different pH.

3.3. Effect of the Enzyme on Acrylamide Formation in French Fries and Bread under Controlled Conditions

Potatoes and flour are two staple foods used to produce fried potatoes and bakery products. In Europe, fried potatoes and bakery products contribute 50% and 20% of humanity's ingestion of acrylamide, respectively [9,11,40,41]. Hence, the degradation of acrylamide content in fried potatoes and bakery products can effectively reduce the daily intake of acrylamide, which is of great significance to a healthy diet. In this study, we investigated the mitigation effect of L-asparaginase on acrylamide formation in common fried potatoes (French fries) and bakery products (bread).

Without enzyme treatment, the acrylamide content in French fries reached 3223 µg/kg. With different concentrations (10, 20, 40, 60, and 80 U/mL) of ECA and its mutant D60W/L211R/L310F, potatoes were, respectively, treated at pH 7.5 and optimum temperatures (ECA 37 °C and D60W/L211R/L310F 45 °C) for 20 min. The mitigation effect on acrylamide formation of French fries is shown in Figure 4A. After treating potatoes with 60 U/mL ECA and its mutant, the acrylamide content in potato chips decreased by 75.5% and 84.1%, respectively; also, the acrylamide content did not further decrease significantly when the enzyme amount was increased to 80 U/mL. For the sake of the production cost, 60 U/mL L-asparaginase was used for the subsequent research.
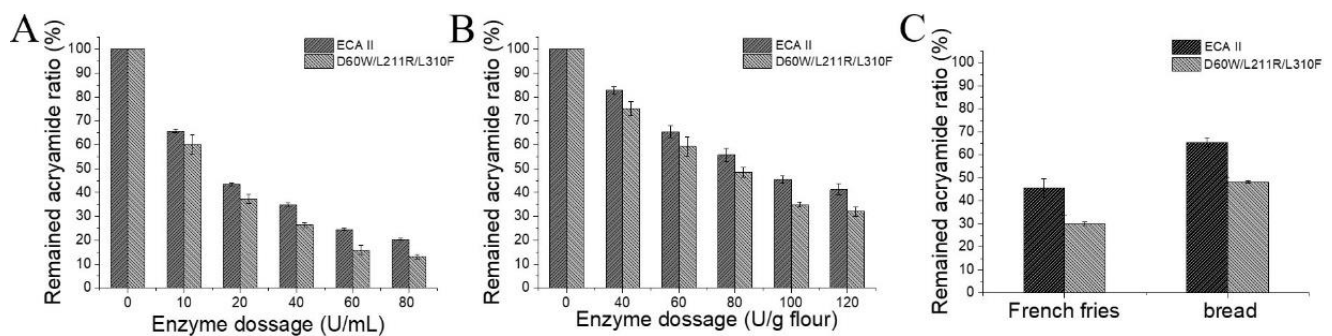

Figure 4. Effect of ECA and its mutation D60W/L211R/L310F on acrylamide formation in French fries and bread. (**A**,**B**) Effect of different concentrations of the enzyme on acrylamide formation in French fries (**A**) and bread (**B**) under optimum conditions. (**C**) Effect of the enzyme on acrylamide formation in French fries and bread under uncontrolled conditions.

To complete the enzyme treatment of the flour, Tris-HCl (50 mM, pH 7.5) containing different concentrations (40, 60, 80, 100, and 120 U/g) of L-asparaginase were used for kneading the dough, and the optimum temperatures (ECA 37 °C and D60W/L211R/L310F 45 °C) of the dough and fermentation were maintained in an incubator. The mitigation effect on acrylamide formation of bread is shown in Figure 4B. Without enzyme treatment, the acrylamide content in the bread reached 931 µg/kg. After treatment with 100 U/g flour ECA and D60W/L211R/L310F, the acrylamide content in the bread decreased by 54.5% and 65.1%, respectively, while the acrylamide content did not further decrease significantly when the enzyme concentration was increased. Hence, in the subsequent research, 100 U/g flour L-asparaginase was used to inhibit acrylamide formation in bread.

Furthermore, compared with the same dose of ECA, the acrylamide content of potato chips and bread treated with D60W/L211R/L310F was further reduced, showing a better application effect, which might be due to the better stability of the mutant and reduced loss of enzyme activity in the pretreatment time. In addition, when the amount of enzyme reached a certain level (60 U/mL in potatoes and 100 U/g in flour), further increasing the enzyme concentration did not reduce the acrylamide content significantly in food (Figure 4A,B). It might be because L-asparagine, which can be contacted with enzymes, was already degraded. Thus, increasing the enzyme amount hardly increased the reaction between enzyme and L-asparagine further and hence did not reduce the subsequent formation of acrylamide. For reducing the formation of acrylamide in food using the

enzyme in the future, the treatment effect may be strengthened by increasing the contact between the enzyme and food raw materials.

3.4. Effect of the Enzyme on Acrylamide Formation in French Fries and Bread under Uncontrolled Conditions

In practical application, it is difficult to strictly control the reaction temperature and pH as in the laboratory; extensive experiments are more consistent with reality. Therefore, we studied the treatment of potatoes and flour with the enzyme in tap water without controlling the reaction temperature and pH to verify its effect on the degradation of acrylamide in potato chips and bread.

In raw materials, the pH of tap water, potatoes, and flour was 6.5, 7.3, and 6.4, respectively. Potatoes and flour were treated with 60 U/mL and 100 U/g flour, respectively, and the residual acrylamide content of French fries and bread was measured (Figure 4C). Compared with the treatment under constant-temperature and constant-pH conditions (Figure 4A,B), the effect of enzyme treatment decreased due to the lack of the optimal conditions. The acrylamide in French fries and bread treated with D60W/L211R/L310F decreased by 69.9% and 51.7%, respectively, which was 27% and 49.9% higher than that of the wild type. Due to the lack of a buffer solution and temperature control, the temperature and pH of the treatment were not constant, while the working temperature and pH of the mutant were wider and more stable, meeting the application requirements, so the mutation had a better application effect than that of the wild type and exhibited a great application potential.

4. Conclusions

Through MD simulation and mutation of *E. coli* L-asparagine, we obtained a mutant with wider application temperature and pH and better stability, verifying the effect of acrylamide control in French fries and bread. Without controlled treatment temperature and pH, the mutant could reduce the acrylamide content in French fries and bread by 69.9% and 51.7%, respectively, with 60 U/mL and 100 U/g flour enzyme, and showed the potential to reduce food acrylamide formation in practical applications.

References

1. Cunha, M.C.; Dos Santos Aguilar, J.G.; de Melo, R.R.; Nagamatsu, S.T.; Ali, F.; de Castro, R.J.S.; Sato, H.H. Fungal L-asparaginase: Strategies for production and food applications. *Food Res. Int.* **2019**, *126*, 108658. [CrossRef]
2. Wang, Y.; Wu, H.; Zhang, W.; Xu, W.; Mu, W. Efficient control of acrylamide in French fries by an extraordinarily active and thermo-stable l-asparaginase: A lab-scale study. *Food Chem.* **2021**, *360*, 130046. [CrossRef]
3. Exon, J.H. A review of the toxicology of acrylamide. *J. Toxicol. Environ. Health B Crit. Rev.* **2006**, *9*, 397–412. [CrossRef] [PubMed]
4. Daniali, G.; Jinap, S.; Hajeb, P.; Sanny, M.; Tan, C.P. Acrylamide formation in vegetable oils and animal fats during heat treatment. *Food Chem.* **2016**, *212*, 244–249. [CrossRef]
5. Anese, M.; Nicoli, M.C.; Verardo, G.; Munari, M.; Mirolo, G.; Bortolomeazzi, R. Effect of vacuum roasting on acrylamide formation and reduction in coffee beans. *Food Chem.* **2014**, *145*, 168–172. [CrossRef]
6. Zhu, Y.; Luo, Y.; Sun, G.; Wang, P.; Hu, X.; Chen, F. Role of glutathione on acrylamide inhibition: Transformation products and mechanism. *Food Chem.* **2020**, *326*, 126982. [CrossRef]
7. Khalil, N.M.; Rodríguez-Couto, S.; El-Ghany, M.N.A. Characterization of Penicillium crustosum l-asparaginase and its acrylamide alleviation efficiency in roasted coffee beans at non-cytotoxic levels. *Arch. Microbiol.* **2021**, *203*, 2625–2637. [CrossRef]
8. Kukurová, K.; Morales, F.J.; Bednáriková, A.; Ciesarová, Z. Effect of L-asparaginase on acrylamide mitigation in a fried-dough pastry model. *Mol. Nutr. Food Res.* **2009**, *53*, 1532–1539. [CrossRef]
9. Jia, R.; Wan, X.; Geng, X.; Xue, D.; Xie, Z.; Chen, C. Microbial L-asparaginase for Application in Acrylamide Mitigation from Food: Current Research Status and Future Perspectives. *Microorganisms* **2021**, *9*, 1659. [CrossRef]
10. Bhagat, J.; Kaur, A.; Chadha, B.S. Single step purification of asparaginase from endophytic bacteria Pseudomonas oryzihabitans exhibiting high potential to reduce acrylamide in processed potato chips. *Food Bioprod. Process.* **2016**, *99*, 222–230. [CrossRef]
11. Meghavarnam, A.K.; Janakiraman, S. Evaluation of acrylamide reduction potential of l-asparaginase from Fusarium culmorum (ASP-87) in starchy products. *LWT* **2018**, *89*, 32–37. [CrossRef]
12. Zuo, S.; Zhang, T.; Jiang, B.; Mu, W. Reduction of acrylamide level through blanching with treatment by an extremely thermostable l-asparaginase during French fries processing. *Extremophiles* **2015**, *19*, 841–851. [CrossRef] [PubMed]
13. Shi, R.; Liu, Y.; Mu, Q.; Jiang, Z.; Yang, S. Biochemical characterization of a novel L-asparaginase from Paenibacillus barengoltzii being suitable for acrylamide reduction in potato chips and mooncakes. *Int. J. Biol. Macromol.* **2017**, *96*, 93–99. [CrossRef] [PubMed]
14. Jia, M.M.; Xu, M.J.; He, B.B.; Rao, Z.M. Cloning, Expression, and Characterization of L-Asparaginase from a Newly Isolated Bacillus subtilis B11-06. *J. Agric. Food Chem.* **2013**, *61*, 9428–9434. [CrossRef]
15. Farahat, M.G.; Amr, D.; Galal, A. Molecular cloning, structural modeling and characterization of a novel glutaminase-free L-asparaginase from Cobetia amphilecti AMI6. *Int. J. Biol. Macromol.* **2020**, *143*, 685–695. [CrossRef] [PubMed]
16. Hendriksen, H.V.; Kornbrust, B.A.; Østergaard, P.R.; Stringer, M.A. Evaluating the Potential for Enzymatic Acrylamide Mitigation in a Range of Food Products Using an Asparaginase from Aspergillus oryzae. *J. Agric. Food Chem.* **2009**, *57*, 4168–4176. [CrossRef] [PubMed]
17. Li, X.; Zhang, X.; Xu, S.; Xu, M.; Yang, T.; Wang, L.; Zhang, H.; Fang, H.; Osire, T.; Rao, Z. Insight into the thermostability of thermophilic L-asparaginase and non-thermophilic L-asparaginase II through bioinformatics and structural analysis. *Appl. Microbiol. Biotechnol.* **2019**, *103*, 7055–7070. [CrossRef]
18. Zhang, J.; Xu, M.; Ge, X.; Zhang, X.; Yang, T.; Xu, Z.; Rao, Z. Reengineering of the feedback-inhibition enzyme N-acetyl-l-glutamate kinase to enhance l-arginine production in Corynebacterium crenatum. *J. Ind. Microbiol. Biotechnol.* **2017**, *44*, 271–283. [CrossRef]
19. Li, X.; Zhang, X.; Xu, S.; Zhang, H.; Xu, M.; Yang, T.; Wang, L.; Qian, H.; Zhang, H.; Fang, H.; et al. Simultaneous cell disruption and semi-quantitative activity assays for high-throughput screening of thermostable L-asparaginases. *Sci. Rep.* **2018**, *8*, 7915. [CrossRef]
20. Roberts, J.; Burson, G.; Hill, J.M. New Procedures for Purification of l -Asparaginase with High Yield from *Escherichia coli*. *J. Bacteriol.* **1968**, *95*, 2117–2123. [CrossRef]
21. Lubkowski, J.; Wlodawer, A. Geometric considerations support the double-displacement catalytic mechanism of l -asparaginase. *Protein Sci.* **2019**, *28*, 1850–1864. [CrossRef] [PubMed]
22. Alexander, N.; Woetzel, N.; Meiler, J. Bcl::Cluster: A method for clustering biological molecules coupled with visualization in the Pymol Molecular Graphics System. In Proceedings of the 2011 IEEE 1st International Conference on Computational Advances in Bio and Medical Sciences (ICCABS), Orlando, FL, USA, 3–5 February 2011; Volume 2011, pp. 13–18. [CrossRef]
23. Jiménez-Osés, G.; Osuna, S.; Gao, X.; Sawaya, M.; Gilson, L.; Collier, S.J.; Huisman, G.W.; Yeates, T.O.; Tang, Y.; Houk, K.N. The role of distant mutations and allosteric regulation on LovD active site dynamics. *Nat. Chem. Biol.* **2014**, *10*, 431–436. [CrossRef] [PubMed]
24. Boehr, D.D.; Nussinov, R.; Wright, P.E. The role of dynamic conformational ensembles in biomolecular recognition. *Nat. Chem. Biol.* **2009**, *5*, 789–796. [CrossRef] [PubMed]
25. Boehr, D.D.; Dyson, H.J.; Wright, P.E. An NMR Perspective on Enzyme Dynamics. *Chem. Rev.* **2006**, *106*, 3055–3079. [CrossRef]
26. Alley, E.C.; Khimulya, G.; Biswas, S.; AlQuraishi, M.; Church, G.M. Unified rational protein engineering with sequence-based deep representation learning. *Nat. Methods* **2019**, *16*, 1315–1322. [CrossRef]
27. Lindorff-Larsen, K.; Piana, S.; Palmo, K.; Maragakis, P.; Klepeis, J.L.; Dror, R.O.; Shaw, D.E. Improved side-chain torsion potentials for the Amber ff99SB protein force field. *Proteins Struct. Funct. Bioinform.* **2010**, *78*, 1950–1958. [CrossRef]

28. Hess, B.; Kutzner, C.; van der Spoel, D.; Lindahl, E. GROMACS 4: Algorithms for Highly Efficient, Load-Balanced, and Scalable Molecular Simulation. *J. Chem. Theory Comput.* **2008**, *4*, 435–447. [CrossRef]

29. Xia, Y.; Cui, W.; Cheng, Z.; Peplowski, L.; Liu, Z.; Kobayashi, M.; Zhou, Z. Improving the Thermostability and Catalytic Efficiency of the Subunit-Fused Nitrile Hydratase by Semi-Rational Engineering. *ChemCatChem* **2018**, *10*, 1370–1375. [CrossRef]

30. Phillips, J.C.; Braun, R.; Wang, W.; Gumbart, J.; Tajkhorshid, E.; Villa, E.; Chipot, C.; Skeel, R.D.; Kalé, L.; Schulten, K. Scalable molecular dynamics with NAMD. *J. Comput. Chem.* **2005**, *26*, 1781–1802. [CrossRef]

31. Swain, A.L.; Jaskolski, M.; Housset, D.; Rao, J.K.M.; Wlodawer, A. Crystal-Structure of *Escherichia coli* L-Asparaginase, an Enzyme Used in Cancer-Therapy. *Proc. Natl. Acad. Sci. USA* **1993**, *90*, 1474–1478. [CrossRef]

32. Tomar, R.; Sharma, P.; Srivastava, A.; Bansal, S.; Ashish; Kundu, B. Structural and functional insights into an archaeal L-asparaginase obtained through the linker-less assembly of constituent domains. *Acta Crystallogr. Sect. D Biol. Crystallogr.* **2014**, *70*, 3187–3197. [CrossRef] [PubMed]

33. Miller, M.; Rao, J.K.M.; Wlodawer, A.; Gribskov, M.R. A Left-Handed Crossover Involved in Amidohydrolase Catalysis—Crystal-Structure of Erwinia-Chrysanthemi L-Asparaginase with Bound L-Aspartate. *FEBS Lett.* **1993**, *328*, 275–279. [CrossRef]

34. Zhou, J.; Zhang, R.; Yang, T.; Liu, Q.; Zheng, J.; Wang, F.; Liu, F.; Xu, M.; Zhang, X.; Rao, Z. Relieving Allosteric Inhibition by Designing Active Inclusion Bodies and Coating of the Inclusion Bodies with Fe3O4 Nanomaterials for Sustainable 2-Oxobutyric Acid Production. *ACS Catal.* **2018**, *8*, 8889–8901. [CrossRef]

35. Yang, B.; Wang, H.; Song, W.; Chen, X.; Liu, J.; Luo, Q.; Liu, L. Engineering of the Conformational Dynamics of Lipase to Increase Enantioselectivity. *ACS Catal.* **2017**, *7*, 7593–7599. [CrossRef]

36. Brosnan, M.P.; Kelly, C.T.; Fogarty, W.M. Investigation of the Mechanisms of Irreversible Thermoinactivation of Bacil-lus-Stearothermophilus Alpha-Amylase. *Eur. J. Biochem.* **1992**, *203*, 225–231. [CrossRef]

37. Vidya, J.; Ushasree, M.V.; Pandey, A. Effect of surface charge alteration on stability of l-asparaginase II from *Escherichia* sp. *Enzym. Microb. Technol.* **2014**, *56*, 15–19. [CrossRef]

38. Niu, C.; Zhu, L.; Xu, X.; Li, Q. Rational Design of Disulfide Bonds Increases Thermostability of a Mesophilic 1,3-1,4-beta-Glucanase from Bacillus terquilensis. *PLoS ONE* **2016**, *11*, e0154036. [CrossRef]

39. Long, S.; Zhang, X.; Rao, Z.; Chen, K.; Xu, M.; Yang, T.; Yang, S. Amino acid residues adjacent to the catalytic cavity of tetramer l -asparaginase II contribute significantly to its catalytic efficiency and thermostability. *Enzym. Microb. Technol.* **2016**, *82*, 15–22. [CrossRef]

40. Keramat, J.; LeBail, A.; Prost, C.; Jafari, M. Acrylamide in Baking Products: A Review Article. *Food Bioprocess Technol.* **2011**, *4*, 530–543. [CrossRef]

41. Nguyen, H.T.; Van der Fels-Klerx, H.J.; Peters, R.J.B.; Van Boekel, M.A.J.S. Acrylamide and 5-hydroxymethylfurfural formation during baking of biscuits: Part I: Effects of sugar type. *Food Chem.* **2016**, *192*, 575–585. [CrossRef]